High Temp. Mater. Proc., Vol. **30** (2011), pp. 51–61 DOI 10.1515/HTMP.2011.007

Development of Magnesium Powder Metallurgy AZ31 Alloy Using Commercially Available Powders

Paul Burke[1] **and Georges J. Kipouros**[2,*]

[1] Massachusetts Institute of Technology, Department of Materials Science and Engineering, Cambridge, Masachusetts, U.S.A.

[2] Materials Engineering Program, Dalhousie University, Halifax, Nova Scotia, Canada

Abstract. Magnesium and its alloys are attractive materials for use in automotive and aerospace applications because of their low density and good mechanical properties. However, difficulty in forming magnesium and the limited number of available commercial alloys limit their use. The present work reviews the efforts to improve the attractiveness of magnesium through non-traditional processing, and presents the results of producing AZ31 magnesium alloy via powder metallurgy P/M. P/M can be used to alleviate the formability problem through near-net-shape processing, and also allows unique chemical compositions that can lead to the development of new alloys with novel properties.

The feasibility of producing magnesium powder metallurgy products utilizing the industrially dominant process of mixed powder blending, uni-axial die compaction and controlled atmosphere sintering was investigated. An alloy composition based on the commercial Mg alloy AZ31 (3 mass % Al, 1 mass % Zn) was used to facilitate the comparison to similar wrought product. The optimal processing conditions (compaction pressure, sintering time and temperature) were found to maximize sintered density and mechanical properties.

Results show that sintering temperature is one of the major variables that has an appreciable effect on the final properties of the samples, and that the effects of compaction pressure and sintering time were insignificant. The material showed poor tensile properties, with a maximum tensile strength of 32 MPa due to lack of sufficient densification. The latter was related to the lack of liquid phase formed during sintering of Al/Zn magnesium alloys and the barrier to diffusion due to the presence of the stable magnesium surface layer.

Keywords. Magnesium powders, magnesium powder metallurgy, AZ31, sintering phenomena.

PACS®(2010). 81.20.EV, 72.15.-V, 82.40.ck, 82.0.-s, 89.20.kk, 61.66.DK, 66.30.Ny.

1 Introduction

In the past quarter century the increasing cost of energy and increased environmental awareness has lead to a global requirement for the reduction of automotive emissions. One strategy for the reduction of emissions is reducing the gross weight of vehicles. As the weight is decreased, less fuel is consumed to propel the vehicle. The average vehicle in 1977 had a mass of 1666 kg, and in 2001 the average weight had been reduced to 1504 kg; an over 136 kg reduction [1]. One of the principal reasons for the weight reduction was the increased use of lightweight materials, especially aluminum. In the same 24 year period, the average amount of Al utilized per automobile climbed from 44 kg to 116.6 kg. The driving force behind the increased usage can be attributed to the intense research effort put forth to provide over 1600 aluminum alloys from multi-component systems and numerous production and fabrication improvements. More recently, aluminum products processed via powder metallurgy (P/M) routes have shown excellent properties and are increasing in utilization.

Magnesium, which has the lowest density of all structural metals, has not enjoyed the phenomenal increase in average mass per vehicle that aluminum has, but had an exceptional growth of 850 %. Unfortunately, the actual amounts went from under 1 kg in 1977 to 3.86 kg in 2001. Aside for low density, magnesium has a number of other advantageous properties. Its stiffness to weight ratio is very high; one kilogram of magnesium is as stiff as 3.96 kg of aluminum and 4.62 kg of steel. The dimensional stability and damping capacity are high, it is easily machined and can be readily recycled [2]. For magnesium to penetrate the automotive industry as a structural material several requirements need to be met [3].

Magnesium has poor corrosion resistance due to heavy metal contamination [4] and lacks a catalogue of developed alloys [5]. The use of magnesium in under the hood components is also hindered by the low creep resistance of commercial alloys [2]. Also, magnesium has a hexagonal close packed (HCP) crystal structure, which leads to difficulty in forming, especially at room temperature [5].

Industrially, one of the most commonly utilized magnesium alloys is AZ31, which contains 3 % aluminum and

Corresponding author: Georges J. Kipouros, Materials Engineering Program, Dalhousie University, 1360 Barrington Street, Halifax, Nova Scotia, Canada B3J 2X4; E-mail: georges.kipouros@dal.ca.

Received: May 23, 2010. Accepted: August 5, 2010.

1 % zinc, by weight. It is used to produce wrought products such as sheet and plate, as well as extruded bars and shapes. The relatively low Al content allows greater ductility at hot working temperatures, and also strengthens the matrix by solid solution. The phase diagram suggests that precipitation hardening may be possible because Al solubility reduces from a maximum of 12.7 mass % to 2 mass % at room temperature. However, the precipitates formed, $Mg_{17}Al_{12}$ intermetallics, are coarse and not dense enough to produce a strong strengthening effect.

Zinc is added to magnesium aluminum alloys in small amounts to further increase strength by solid solution. Zinc will form beneficial precipitates through age hardening, but the co-precipitation of the $Mg_{17}Al_{12}$ intermetallic negates any increase in strength. AZ31 alloy is generally considered non-heat treatable.

Powder metallurgy can be used to alleviate one the largest problems with magnesium utilization, formability, with its inherent near-net-shape processing. Raw magnesium powders of a 75 μm typical size are blended with alloying elements and compacted in a die at high pressure. The "green" compacts are then sintered in a controlled atmosphere at a temperature lower than the melting point, but high enough to allow rapid diffusion between the powder particles. The method in which powders are produced allows unique chemical compositions that can lead to new alloys with novel properties [6, 7].

Limited research has been done on the use of powder metallurgy routes for the production of magnesium products. The research that has involved magnesium powder mainly uses P/M as a means to produce difficult to form alloys. These include metal matrix composites (MMC) [8–10], where P/M can alleviate some of the matrix/reinforcement interface issues when the matrix metal is in the molten state. The P/M method also allows a highly homogenous mixture of the reinforcement particles within the matrix, resulting in consistent mechanical properties in all directions. Difficulty to achieve successful sintering has brought into question the possibility of P/M to produce magnesium matrix composites [9]. The state in which the surface of the magnesium powder before the P/M processing is the controlling factor in the sintering process. Obviously the methods of production of magnesium powder are critical in achieving the properties required for a successful sintering. It appears that no attention has been paid into the characterization of the surface properties of the magnesium powders.

The other major research focus is the use of nano-sized base powders to produce a very fine grain structure in the final sintered product. With the greatly reduced grain size as compared to parts produced through ingot metallurgy, the strength and superplastic properties of the metal is proportionally increased [11]. Powders of alloys that contain rare earth elements and other additions are produced by atomization, where rapid solidification allows extended solubility not possible with ingot metallurgy. Alloying additions are chosen to improve strength, creep resistance and superplasticity [12].

The P/M method utilized to produce the majority of samples in both the MMC and grain refinement research is through canned powder hot extrusion [11, 12] primarily due to safety considerations. In this process, the base powders are blended and loaded into a thin-walled cylindrical vessel made from a highly formable metal such as aluminum or copper. The powders are vacuum de-gassed at an elevated temperature to remove air trapped between particles. Following de-gassing, the can is sealed. Extrusion takes place at sintering temperature and the reduction is typically between 10 : 1 and 20 : 1, allowing the powders to be compacted and sintered in one step. This process produces parts with very high densities, in the range of 98 %+, but it is mainly a laboratory batch type procedure. To implement such a process on an industrial scale would be both costly and time consuming. It also forfeits near-net-shape processing, one of P/Ms key advantages.

The major issue in the development of the magnesium P/M is the availability of commercial magnesium powders. Unlike aluminum most commercial magnesium powders are produced by mechanical grinding. The low cost and less restrictive requirements for the main intended use of magnesium as a reactant make grinding attractive. For P/M applications the angular morphology of the powder gives good green strength because of mechanical interlocking, but the powder particles are typically covered by a thick surface layer. The layer is hypothesized to contain primarily oxides, but hydroxides and carbonates are possible due to long subjection to atmospheric conditions during the grinding process. Recently magnesium powder is also being produced commercially by centrifugal atomization by a small number of companies. The product has very little surface oxidation due to the inert conditions maintained during production, but the spherical morphology gives poor green strength. Because the amount of surface absorbed oxygen is not readily available the applicability of powder metallurgy to magnesium metal is in question [9]. No fundamental studies of the sintering behaviour of magnesium powders have been completed to date, but preliminary studies have been reported [13, 14]. The goal of the study is to determine if the surface layer is in fact the main obstacle to producing magnesium P/M parts without the addition of secondary hot working, by looking solely at solid state sintering of pure magnesium powders. A new technique, focused ion beam/transmission electron microscopy (FIB/TEM), was applied to identify the nature of the surface layer [15] with very encouraged results.

A way to bypass the oxide layer is by creating cracks and pores through it. During compaction, the force exerted on the powder is enough to break the layer, creating short circuit pathways for unimpeded sintering. Also, during heating of the powder, any hydroxide or carbonate that is part

of the layer will decompose, which will create pores in the layer as gas is released. If there are adjacent cracks or pores in two particles, rapid sintering will take place at that local area. However, if a point contact between particles does not have a break in the layer, diffusion is still impeded.

If the alloying being sintered has one or more low melting point additions, a liquid phase forms during sintering. The liquid flows through the inter-granular space, and if the matrix is soluble in the liquid, the liquid acts as a diffusion bridge between adjacent powder particles. The presence of the liquid phase can make use of cracks or pores in the surface layer that may not have been located at a point contact. Because of this, there are many more areas for diffusion to proceed, and sintering is much more rapid. However, if the liquid is also soluble in the matrix, the liquid phase is termed transient, and will be absorbed into the matrix at some point and can no longer assist sintering.

The objective of this research is to improve the attractiveness of magnesium through non-traditional processing, by producing magnesium alloys via powder metallurgy. The feasibility of producing magnesium powder metallurgy products utilizing the industrially dominant process of mixed powder blending, uni-axial die compaction and controlled atmosphere sintering was investigated, using the most commonly available ground magnesium powder. An alloy composition based on the commercial Mg alloy AZ31 (3 mass % Al, 1 mass % Zn) was used to facilitate comparison to similar wrought products. Alloy AZ31 has been produced through P/M processing previously [16], but with the addition of secondary hot extrusion of the sintered compacts. This work investigated the possibility of utilizing parts as sintered, to take full advantage of net shape forming. The optimal processing conditions (compaction pressure, sintering time and temperature) were determined to maximize sintered density and mechanical properties.

The samples were characterized by determining the dimensional change in the sintered compacts, the theoretical density achieved and the apparent hardness. To further validate the results, the microstructure, chemical composition and tensile behaviour of select samples were be tested.

2 Experimental

2.1 Materials

The commercially available base Mg, Al and Zn powders were supplied by Eckart Granules. Elemental magnesium powder of a rounded morphology with an average size of ∼75 μm was produced by mechanical grinding, while spherical elemental aluminum powder of an average ∼120 μm size and irregularly shaped elemental zinc powder of an average ∼36 μm size were produced by air atomization. The major impurity in all three powders was oxygen. Wax lubricant was added to reduce die wall friction during compaction. All powders were characterized by laser Malvern size analyzer in water to determine the size distribution.

2.2 Sample Preparation

Mixing and Die Lubrication

The proper ratio of each elemental powder was measured and combined with 2 mass % wax lubricant to decrease die wall friction during compaction, and the powders were blended for 30 minutes (= 30× 60 s) in a Turbula shaker-blender.

Pressing/Sintering

The homogenous product of mixing was compacted using a uni-axial frame press equipped with an appropriately designed die to produce rectangular samples measuring 12.7 mm width by 31.7 mm length having a height between 8 and 10 mm. To determine the optimum compaction pressure a compaction curve was produced by pressing the samples at 300, 400 and 500 MPa. Tensile specimens were produced by unixial die compaction (UDC) using a dog-bone shaped die, which produced samples with a 35 mm gauge length and a nominal cross section of 4 mm by 5.75 mm.

Sintering took place in a tube furnace which was first evacuated and then purged several times [17] under a flowing argon atmosphere. The temperature-time sintering diagram of the samples is shown in Figure 1. The uniaxially pressed samples containing mixed lubricant were first heated to 360 °C (= 633 K) and held at this temperature for 30 minutes to completely evaporate any remaining wax lubricant which is transported by the flowing argon and condensed at the cold part of the tube furnace. Following delubrication, the samples were heated to the corresponding sintering temperature, and kept at the sintering temperature for the required time. After sintering, the furnace was turned off and the samples remained in the hot zone until the quenching temperature was reached, at which point the

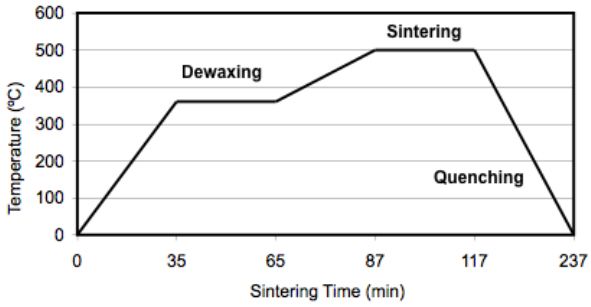

Figure 1. Sintering schematic of uni-axial die compaction samples.

samples were moved into a water cooled jacket and cooled to room temperature.

2.3 Sample Characterization

Density

The density of the material was measured on both the green as well as the sintered products and was determined using the MPIF standard 42 "Density of Compacted or Sintered Powder Metallurgy Products" [18]. This method involved weighing the sample in air, then impregnating the sample with a suitable oil (Nuto H 46) by vacuum impregnation. After the impregnation process, the sample was reweighed in a water bath containing the appropriate amount of PhotoFlo as a wetting agent. The weights of the dried, oil impregnated and suspended in water sample were recorded. Using the formula for MPIF standard 42 [18] the green and sintered densities were determined in g/cc and are reported as percent of the expected theoretical densities.

Microstructure Characterization

Optical micrographs were recorded for as-sintered and polished samples using an Olympus model BH-2 optical microscope equipped with a Nikon digital camera. Further characterization involved the study of the microstructure and phases present in the samples by a Hitachi S-4700 Field Emission Scanning Electron Microscope (FESEM) operating at 5 kV and a current of 10 μA, equipped with energy dispersive spectroscopy (EDS). Samples for SEM analysis were prepared by notching and breaking the part, reveling the fracture surface due to impact. X-ray spectra were obtained using a Bruker AXS, D8 Advance x-ray spectrometer operating with a copper tube at 40 kV and 40 mA. Chemical analysis was also performed on selected samples.

Mechanical Properties

Apparent hardness values were obtained to evaluate the success of the powder metallurgy process. A steel ball indenter (1/8 inch = 3.175 mm) was forced into the surface using an applied load of 60 kgf (= 9.8 × 60 N), corresponding to the Rockwell H scale. To produce a single data point and in order to assess the error, each measurement was repeated 6 times and the results were averaged.

Tensile samples were prepared for select samples and tested using an Instron tensile test bed equipped with flat clamping jaws. Samples were pulled at a rate of 0.01 mm per second until failure. A digital extensometer connected to a computer was used to collect strain data, which were combined with stress data from the test frame to plot stress/strain curves for each sample.

3 Results and Discussion

The first results presented are pertaining to the common variables of P/M processing that must be optimized: compaction pressure, sintering temperature, sintering time and quenching temperature. Supporting results that were not part of the optimization study such as microstructure examination, chemical composition and tensile data are offered in subsequent sections.

Because this study is unique in determining the properties of a structural magnesium alloy produced without the aide of secondary hot work to further densify the samples, there are a limited number of results in the literature from which to compare. Comparison was instead made between the P/M AZ31 alloy samples produced and its equivalent wrought (extruded) AZ31 alloy.

3.1 Base Powders

The base magnesium powder is known to have been manufactured by mechanical grinding. The morphology of the powder is shown in Figure 2. The Mg powder, as well as the Al and Zn were first tested for chemical composition. Table 1 lists the elements present.

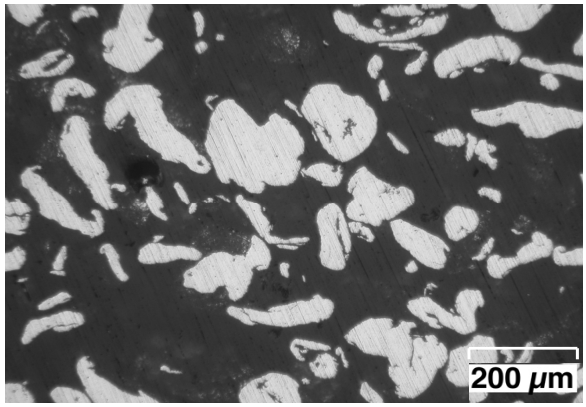

Figure 2. Optical micrograph of as received ground pure magnesium powder.

	Mass Percent		
	Magnesium	**Aluminum**	**Zinc**
Element			
Mg	98.6		
Al		99.5	
Zn			99.8
O	1.32	0.05–0.5	0.2 max
Other	0.08	0–0.45	

Table 1. Chemical composition of base powders used to form P/M AZ31 alloy, as reported by the manufacturer.

3.2 Effect of Compaction

It is important to know the density of the samples before sintering, so that comparisons can be made between the green and sintered state. Figure 3 shows the average theoretical green density of the AZ31 alloy samples as a function of compaction pressure. It can be seen that as the compaction pressure increases so does the resulting green density. However, the effect is decreased at higher compaction pressures and a point is reached where increasing the compaction pressure further does not give a significant increase in green density. Also, increasing compaction pressure increases the time required to compact a sample, increases the wear on tooling and increases the probability of tool jamming. It was decided for this study to test compaction pressures of 300, 400 and 500 MPa to determine any benefits to using an increased compaction pressure, or if a lower compaction pressure would produce acceptable results while relieving the aforementioned problems.

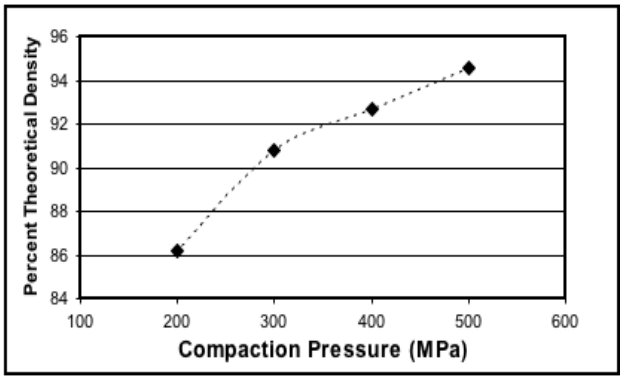

Figure 3. Effect of compaction pressure on green density of AZ31 magnesium alloy.

Dimensional Change

With high compaction pressures the samples are in a highly stressed state. After sintering the amount of work introduced to the powders may cause a change in dimension as the high temperature allows dislocations to rearrange into a lower stress pattern. Because of this rearrangement, some small change in physical size is possible. The samples compacted to 500 MPa showed an average of 0.5 % increase in maximum dimensional change with a result of 2.2 %. The change is very small and perhaps negligible, but the steadily increasing slope may indicate the more highly stressed samples undergo some stress relief during sintering.

Density

It is expected that a sample that exhibits a high density in the green state will also exhibit a high density after sintering, and the samples compacted to a higher pressure do show a slightly higher final density. Increasing the compaction pressure will have the effect of disrupting any surface layers on the powder particles. These layers are effective barriers to diffusion and can also disrupt the wetting and flow of the liquid phase. It can be seen that increasing the compaction pressure increases the final density, possibly due to more interparticle bonding from a reduced surface barrier. The 500 MPa sample had a average density of 89 %, with a decrease of only 0.30 % for the 300 MPa samples, which may indicate that most of the surface layer is disrupted at all compaction pressures, or that the layer remains at all compaction pressures. It is unclear when considering only this result. However, in practice there is no real advantage to higher compaction pressure in terms of sintered density. It is interesting that the final densities of all samples are so close, as the green densities vary by up to 4 %. This is an indication that all effects of the stress introduced during compaction are erased through rearrangement and that the behaviour of the liquid phase formed has more effect on the density than the solid state densification of the magnesium matrix.

Hardness

If the samples were not too fragile to test in the green state, it would be expected that the higher compaction pressure would result in a higher apparent hardness due to work hardening. After sintering, one might expect the same result, but as discussed in the previous section, it is likely that sintering allows for stress relief of the magnesium matrix. The average hardness for the 500 MPa AZ31 magnesium alloy samples was 74.3 Rockwell H after sintering, and different compaction pressures show a maximum difference of less than 1 point. There is a steady increase in hardness with an increase in the compaction pressures, which may not be significant in the overall result, but does show that the small increase in sintered density that occurs with increasing compaction pressure allows for an increase in hardness. In comparison, a wrought AZ31 alloy sample was tested and found to have a hardness of 85 on the Rockwell H scale.

3.3 Effect of Sintering Temperature

Sintering temperature has the largest effect on the behaviour of solid and liquid state densification during sintering. In general, a higher sintering temperature increases the diffusion rate and allows densification to occur more rapidly. For solid state sintering where there is no liquid phase to act as a diffusion bridge, a high sintering temperature is important to achieving significant densification due to the lower number of pathways for diffusion. When a liquid phase is present a higher temperature is also beneficial because there are more diffusion pathways and a higher rate of diffusion.

In the case of the AZ31 alloy a sintering temperature above 420 °C will melt the zinc present and initiate a liquid

phase. At 437 °C and 450 °C, intermetallic phases of magnesium and aluminum that may be present will melt and add volume to the liquid phase. Since all the components of the liquid phase are soluble in the magnesium matrix, it can be assumed that the liquid phase readily wets the matrix grains and a transient type liquid phase results. Therefore, at some point the liquid phase that is assisting densification will be absorbed into the matrix grains. After absorption of the liquid phase, any further densification is limited to solid state diffusion. This presents a case where high temperature and high rates of diffusion may be counter-productive. Therefore it is necessary to determine whether the higher overall diffusion rate that occurs at a higher temperature is more beneficial than a slower overall diffusion rate that allows the liquid phase and increased number of diffusion pathways to persist longer.

Dimensional Change

Typically, an alloy system that displays a persistent liquid phase will show shrinkage after sintering. In the case of a transient liquid phase the components of the liquid are absorbed into the matrix grains increasing their volume. As more of the liquid phase is absorbed, the dimensions of the sample will increase. As can be seen in Figure 4, this is exactly the case in the P/M AZ31 alloy. The dimensional change data depicted in Figure 4 is independent of the other sintering variables of compaction, time and quench temperature. The result is a swelling of more than 3 % in the maximum dimension at 600 °C. At the lowest temperature, the liquid phase persists long enough to allow sufficient densification before being absorbed to counteract the porosity after it is absorbed, and results in slightly over 1 % swelling. It is also possible that the liquid phase is not as completely absorbed as in the 600 °C case, and that at 500 °C the liquid persists and freezes at the matrix grain boundaries once the samples are quenched, reducing the residual porosity.

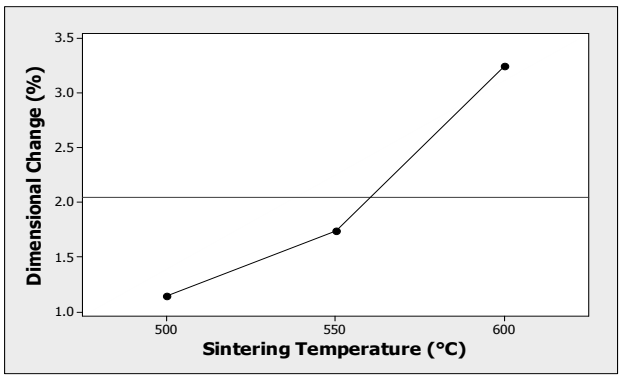

Figure 4. Effects of sintering temperature on the dimensional change of AZ31 magnesium alloy.

3.3.1 Density

As shown in Figure 5, which is independent of the other sintering variables, the maximum difference in density 3.5 %. Similarly to the effect of sintering temperature on dimensional stability, the final density of the samples sintered at a lower temperature exhibit improved results. The affect of a more persistent liquid phase allowing for more diffusion pathways for a longer period that occurs at 500 °C produces increased density even though the rate of diffusion is lower. If the liquid phase is not completely absorbed at 500 °C, the frozen liquid phase will reduce the amount of porosity at the grain boundaries.

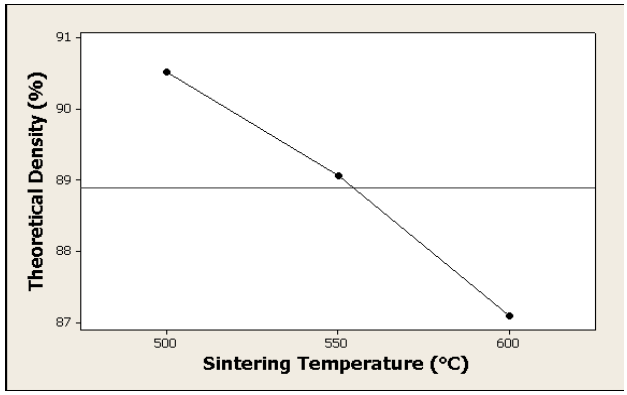

Figure 5. Effects of sintering temperature on the density of AZ31 magnesium alloy.

Increasing the sintering temperature has the conflicting result of increasing the diffusion coefficients and thus increasing the diffusion rate but also reduces the number of diffusion pathways by allowing the liquid phase to be absorbed more quickly, which is more detrimental to the final density than having an increased rate of diffusion at the higher temperature.

Hardness

As expected, the increase in density afforded at lower sintering temperatures increases the hardness of the samples, as shown in Figure 6, which is independent of the other sintering variables. The 3.5 % increase in theoretical density translates into a 5 point hardness increase on the Rockwell H scale. It can be concluded that maximizing the density by sintering at 500 °C has the greatest overall affect on the hardness of the samples.

3.4 Effect of Sintering Time

Next to sintering temperature, the time at which the samples are held at that temperature is the most important consideration. In the case of the AZ31 magnesium alloy and its transient liquid phase, the sintering time will affect the total time in which diffusion can take place in either solid or

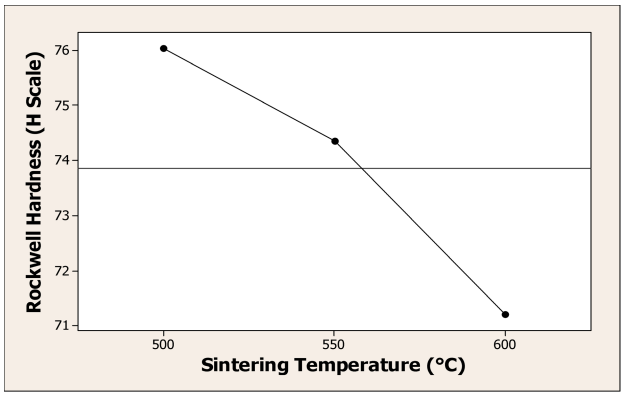

Figure 6. Effects of sintering temperature on the hardness of AZ31 magnesium alloy.

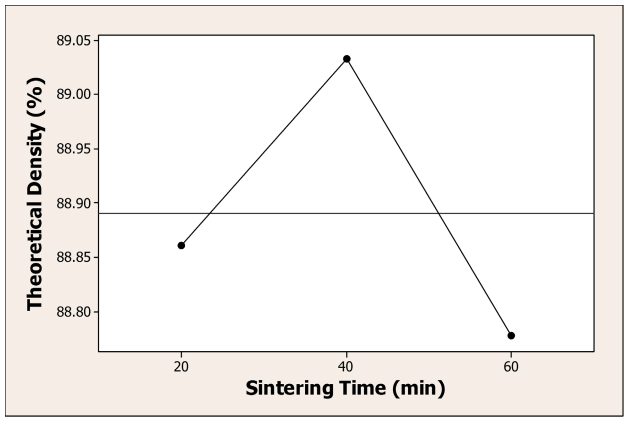

Figure 7. Effects of sintering time on sintered density of AZ31 magnesium alloy.

liquid state, and also the time available for the liquid phase to be absorbed into the magnesium matrix. Therefore there is an interaction between the sintering time and temperature that determines the behaviour of the liquid phase. For example, if the sintering temperature was low but the time long, the liquid phase will persist long enough to densify the samples to a high extent, but there is also sufficient time to allow the liquid phase to be absorbed into the matrix. This will produce an intermediate case where densification was high but residual porosity exists because the liquid phase was absorbed.

Dimensional Change

The resulting dimensional change in the sintered AZ31 magnesium alloy samples due to sintering time was a negligible 0.15 % between the three sintering times, where the 60 minute sintering time is superior at 1.9 %. The 60 minute sintering time may result in less change in physical size in the samples because increased densification occurs, however the error associated with the measurements may negate any difference between the three sintering times.

Density

The complex interactions that occur between the rate of diffusion and the presence of the liquid phase are apparent in Figure 7, which shows the effects of sintering time on sintered density of AZ31 magnesium alloy. The data in Figure 7 is independent of other sintering variables. At the shortest sintering time of 20 minutes, time does not allow sufficient densification to occur by diffusion producing a lower final density, but there is also less time to absorb the liquid phase, which freezes in the grain boundaries and reduces the amount of residual porosity. At the longest sintering time of 60 minutes, there is an increased period in which densification may occur, but also the increased time facilitates the absorption of the liquid phase into the matrix. The result is enough residual porosity that the final density is slightly lower than the 20 minute case, even with the increased densification.

At an intermediate time of 40 minutes, a peak is found where the sintering time is long enough to allow sufficient densification, but short enough that the residual porosity formed when the liquid phase was absorbed is low. This combination results in a small increase in density at 40 minutes, but still only 0.27 % better than the worst case. It can be concluded then that sintering time may have a large effect on the behaviour of the liquid phase and densification, but the resulting net effect on final density is almost negligible.

Hardness

Unlike dimensional change and density where a peak was found at the intermediate sintering time, the shortest time produces a higher hardness of AZ31 magnesium alloy at 74.5 HRH. There is also a non-negligible difference between the measurements with a maximum of 1.6 points, and a steady increase in hardness as sintering time decreases. Unlike previous sections where the hardness can be explained primarily because of higher density, this is not the case with sintering time. Therefore, the explanation must be related to the amount of liquid phase components frozen at the grain boundaries after quenching.

At the shortest sintering time of 20 minutes, there is a greater portion of the liquid phase that has not been absorbed into the magnesium matrix, which then freezes when the sample is quenched. The liquid phase consists of mainly intermetallic phases which are harder than the magnesium matrix. Having the hard intermetallics surrounding the matrix grains would increase the apparent hardness of the sample resulting in a higher hardness for the samples sintered for a shorter time. However, this increase in hardness is likely not beneficial because the grain boundaries are now brittle and a likely place for cracks to initiate and easily spread.

Microstructural examination

Select samples were chosen to be examined by metallography based on the results from the optimization study. Because the effects due to compaction pressure were shown to be negligible, they will not be considered. The microstructural differences will not be visible between samples that show a very small change, such as the maximum density difference of 0.30 % in the case of compaction pressure. In the case of sintering time and temperature, increasing either will effectively increase the amount of the liquid phase that is absorbed by the matrix magnesium. Evidence of frozen liquid phase should be apparent in samples with low sintering time and temperature.

Effect of Sintering Time and Temperature on Microstructure

The micrograph in Figure 8 shows a sample that was sintered at 500 °C for 20 minutes, the lowest combination of time and temperature. The sample has been broken by impact, and Figure 8 is the resulting fracture surface. Individual grains can be seen, and the edges of these grains appear more angular than the original powder as shown in Figure 2, due to deformation during compaction. A higher magnification micrograph of the same sample is shown in Figure 9, which is also an impact fracture surface. The rough, angular surface, which indicates brittle failure, can be seen across the entire fracture surface. The matrix Mg is relatively ductile, but the intermetallic phases that may have frozen at the grain boundaries are hard and brittle. Therefore it can be concluded that fracture occurred through the brittle intermetallic phases that were frozen along the grain boundaries. Figure 10 is an optical micrograph of a sample processed similarly, but cross-sectioned and polished, not fractured. The light grey liquid phase can be seen frozen inside many of the pores and along grain boundaries.

Figure 11 and Figure 12 show the fracture microstructure of a sample that was sintered at 600 °C for 60 minutes, the highest combination of time and temperature. As can be seen in the micrographs, the individual grains of magnesium are less apparent and the degree of bonding between particles is increased. There is no evidence of the frozen liquid phase at the grain boundaries. The fracture surface is smoother, with rounded tops of grains visible, than the

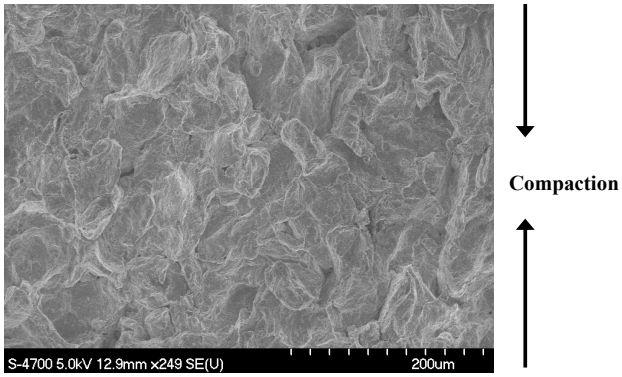

Figure 8. Low magnification SEM micrograph of P/M AZ31 alloy sintered at 500 °C (500 MPa, 20 min, 450 °C).

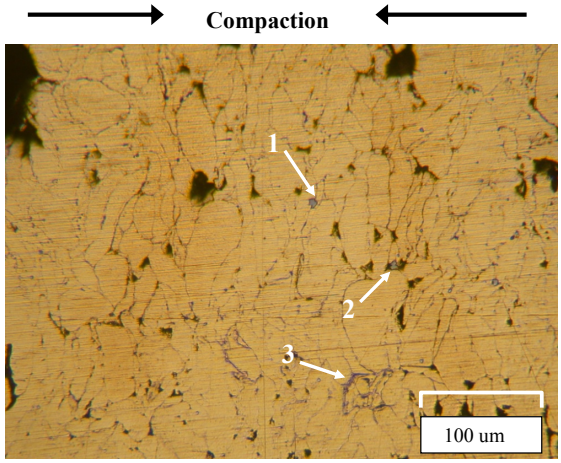

Figure 10. Optical micrograph of P/M AZ31 alloy sintered at 500˚C (500 MPa, 20 min, 450 °C). Arrows indicate light grey areas of frozen liquid phase inside porosity (1, 2), and along grain boundaries (3).

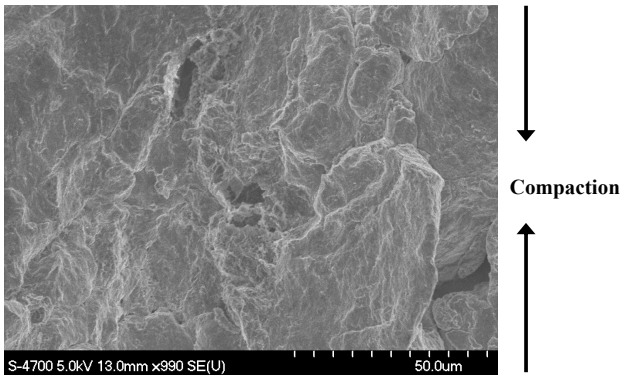

Figure 9. Higher magnification SEM micrograph of P/M AZ31 alloy sintered at 500 °C (500 MPa, 20 min, 450 °C).

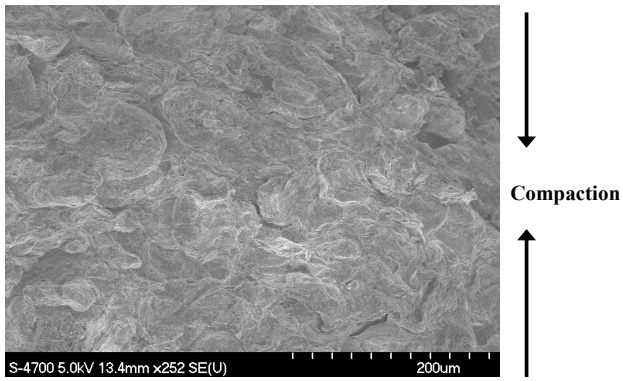

Figure 11. ow magnification SEM micrograph of P/M AZ31 alloy sintered at 600 °C (500 MPa, 60 min, 375 °C).

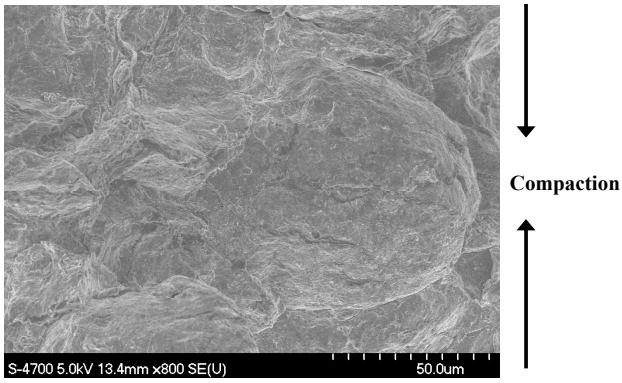

Figure 12. Higher magnification SEM micrograph of P/M AZ31 alloy sintered at 600 °C (500 MPa, 60 min, 375 °C).

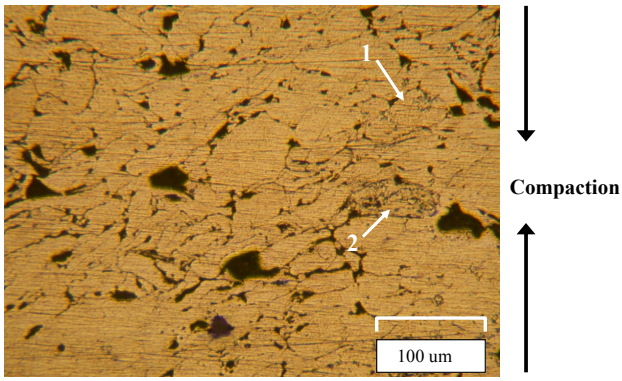

Figure 13. Optical micrograph of P/M AZ31 alloy sintered at 600 °C (500 MPa, 60 min, 375 °C). Arrows indicate light grey areas of frozen liquid phase inside porosity (1, 2).

samples sintered at low time and temperature. This would indicate a more ductile mode of fracture, due to the absence of the brittle intermetallic phases at the grain boundaries.

Figure 13 is an optical micrograph of a sample similarly processed, where the increased porosity is evident, and some increase in interparticle bonding can be seen when compared to Figure 10. There is some small amount of frozen liquid phase apparent inside pores, but in much lesser size and quantity. There is no frozen liquid phase visible between grain boundaries.

3.5 Chemical Composition

Select samples were tested for chemical composition using the EDS equipment on the FESEM. The two samples from the previous section, one with the low extreme of sintering time and temperature (LOW) and the other with the extreme high sintering time and temperature (HIGH), were tested. The results are shown in Table 2, along with the chemical analysis provided for the pure magnesium base powder as it was provided by the manufacturer, and the composition of the base powder as determined by EDS. Also included is the EDS composition of a sample prepared from Mg powder with no alloying additions, which was compacted at 500 MPa, sintered for 60 minutes at 500˚C and quenched immediately following sintering.

The as received powder and the pure Mg sintered compact were also tested by x-ray diffraction. In both cases, the resulting peaks were all characteristic of pure magnesium, with no other un-accounted for peaks. The pure Mg sintered samples were chosen for x-ray analysis as opposed to the P/M AZ31 samples to ensure that oxide peaks would not be masked by the peaks of aluminum, zinc and any related intermetallics.

It can be seen that the level of oxygen in the samples tested by EDS is higher than that reported by the manufacturer. It may be oxidation of Mg during shipping and storage of the base powder, but it seems sintering does not increase the amount of Mg oxidized, as the amount is fairly constant between the as received powder and sintered samples.

3.6 Tensile Behaviour

As with the previous section, the results of the optimization study were used to select which conditions to use to determine mechanical behaviour through tensile testing. Because the effect of the compaction pressures was shown to be negligible, they will not be considered. Also, because a clear advantage was found for the 500 °C sintering temperature with an increase in dimensional stability, density and hardness, only that condition will be considered. The optimization study was somewhat inconclusive in regard to the sintering time variable, as it was the only result that did not produce a linear relationship. Therefore, the tensile testing will focus on the effect of sintering temperature.

Table 3 shows the results of the tensile tests performed on P/M AZ31 dog bone samples compacted at 500 MPa, sintered at 500 °C and quenched at 450 °C. Results are an average of three samples, and associated errors are shown in the table. The table also includes tensile data for a comparable wrought alloy. As with the results for the optimization study, the relationship between the three sintering times is not linear for the ultimate tensile strength and elastic modulus, and peaks at the intermediate time of 40 minutes. The percent elongation of the tensile samples is also inverse to the hardness results obtained in the optimization study, with the 60 minute time showing the highest ductility, and the 20 and 40 minute being similarly low.

This result supports the conclusion from the optimization study that the extent of diffusion and interparticle bonding is balanced with the absorption of the liquid phase. With a sintering time of 40 minutes, the liquid phase is present long enough to promote diffusion and interparticle bonding. The amount of liquid absorbed by the matrix is enough to decrease the amount of brittle intermetallic frozen at the grain

	Mass Percent				
	Powder (Man)	**Powder**	**Pure Mg**	**LOW**	**HIGH**
Element					
Mg	98.6	92.95	92.53	86.04	86.82
Al				3.65	3.67
Zn				1.31	1.96
O	1.32	7.05	7.47	9	7.54

Table 2. Chemical composition of as received powder and sintered compacts. Powder (Man) is the chemical analysis provided by the manufacturer of the Mg powder. Powder is the Mg powder composition determined by EDS. Pure Mg was an un-alloyed sample compacted at 500 MPa, sintered at 500 °C for 60 min, quenched at 500 °C. LOW is P/M AZ31 alloy compacted at 500 MPa, sintered at 500 °C for 20 min, quenched at 450 °C. HIGH is P/M AZ31 alloy compacted at 500 MPa, sintered at 600 °C for 60 min, and quenched at 450 °C.

	Sintering Time			
	20 Minutes	**40 Minutes**	**60 Minutes**	**Wrought AZ31**
UTS (MPa)	22 ±2.3	32 ±0.95	31 ±4.7	260
Percent Elongation	0.116 ±0.04	0.116 ±0.01	0.120 ±0.02	15
Elastic Modulus (GPa)	25.6 ±1.4	30.4 ±1.5	28.5 ±0.9	45

Table 3. Tensile results of P/M AZ31 alloy. Compaction pressure of 500 MPa, sintering temperature of 500 °C and 450 °C quench temperature. Data for wrought AZ31 alloy for comparison [2].

boundaries but not so much that a large number of pores remain. The percent elongation remained the same at 20 and 40 minutes, but increased at the 60 minute sintering time. This result supports the theory that the intermetallic liquid phase is completely absorbed at this time, as the solid solution of magnesium, aluminum and zinc has a higher ductility than the intermetallic liquid phase.

Compared to the wrought AZ31 alloy, the tensile behaviour of the P/M alloy is poor, with a large decrease in ultimate tensile strength, elongation and elastic modulus. The reduction in elongation is expected because of the porosity related with powder metallurgy processing, but most P/M materials have comparable tensile strength with wrought alloys of similar composition. In the case of the P/M AZ31 alloy, the tensile strength is reduced almost by a factor of ten and would not be suitable for any structural application.

The highly soluble, transient liquid phase that forms during sintering may allow for an increased number of interparticle bonds to form by acting as a diffusion bridge between magnesium particles in some processing conditions, but even the best samples show severely reduced tensile strength compared to the wrought alloy. The difference in the amount of liquid phase present may explain differences between the samples produced in this study, but an underlying problem with high porosity and insufficient interparticle bonding are the key issues in comparison with the wrought alloy. Not enough interparticle bonds are formed during sintering to give the samples acceptable strength for structural applications. Therefore, while some processing conditions have shown superior properties, those properties are still not comparable with a wrought product.

Previous work completed in powder metallurgy magnesium alloys has shown that acceptable tensile behaviour is possible, but in these works the sintered compact is further densified by hot extrusion. It may be possible to greatly increase the properties of the P/M AZ31 alloy by using secondary processing such as hot extrusion. Hot working of the samples would increase the density to almost that of the theoretical maximum and the recrytallization that occurs would negate any effects of the liquid phases that formed during sintering. However, by necessitating a secondary operation, the main benefit of P/M products is lost as the compacts will no longer be net shape. Also, the one of the primary reasons for investigating the production of magnesium parts through P/M was to eliminate the need for forming operations. By producing net shape parts, the difficulty of forming HCP structured magnesium is removed.

The limiting factor for producing a successful P/M magnesium alloy may not be the process variables such as compactions pressure, sintering time and temperature and quench temperature, but is linked more to finding alloying elements that will form beneficial liquid phases during sintering. While outside the scope of this work, where commercially available powders were used to produce a P/M alloy of similar composition to a common wrought alloy, future work should include a thorough investigation into possible alloying elements that will form persistent liquid phases that will allow rapid diffusion of magnesium.

4 Conclusions

From the results of the optimization study, it was shown that the effect of the compaction pressure used to form the green samples had a very small bearing on the properties of the sintered samples.

Sintering temperature was shown to have the most marked effect on the properties of the sintered compacts. At low sintering temperature the rate of diffusion through the liquid phase is lower, but the rate of absorption is also low. This allows the liquid phase to persist at the grain boundaries for a longer period, allowing an increased amount of interparticle bonding. The increased bonding results in superior properties.

Statistically, the effect of the sintering time on the final properties of the samples is negligible. While the end result on the dimensional change, density and hardness is low, the sintering time has a large bearing on how the liquid phase formed during sintering behaves. When sintering takes place for the intermediate length of time, a balance is found between the persistence of the liquid phase and the amount of liquid phase that is absorbed. This reduces the hardness somewhat, but since less of the liquid phase is absorbed than at the longer time, less residual porosity will remain and the density of the compacts is higher.

Examining the microstructure of samples sintered at the extremes of time and temperature, the conclusions drawn from the optimization study are reinforced. The brittle intermetallics of the liquid phase can be seen frozen at the grain boundaries of the magnesium matrix particles in the fracture surface of the sample sintered at 500 °C for 20 minutes. In the sample that was sintered at 600 °C for 60 minutes, it was seen that an increased amount of interparticle bonding had occurred, as grain boundaries were less apparent, and there was no evidence of the frozen liquid phase. Therefore it was shown that the liquid phase had been completely absorbed by the magnesium matrix.

The chemical composition of the samples tested by EDS show a high level of oxygen, presumably in the form of MgO. However, the x-ray diffraction results shows no characteristic peaks not associated with pure Mg, indicating the concentration of oxide is low. It is possible that any oxide layer present was sufficiently disrupted and broken by the force of compaction to reduce its negative effect.

The tensile results from the dog bone compacts compacted at 500 MPa, quenched at 450 °C, sintered at 500 °C for 20, 40 and 60 minutes were very poor. As was the case with the design of experiments trial, the results of the tensile tests indicates that the intermediate sintering time of 40 minutes is superior to 20 or 60 minutes. However, the maximum strength achieved was 32 MPa, 228 MPa short of a comparable wrought AZ31 alloy. While a reduced tensile strength is expected because of the residual porosity found in P/M products, the difference found between the P/M AZ31 and wrought alloy show a lack of strong bonds formed during sintering.

Acknowledgments

The authors wish to acknowledge the financial support of the Natural Sciences and Engineering Research Council (NSERC) of Canada, the Minerals Engineering Centre (MEC), and MATNET of Dalhousie University for the use of the characterization equipment.

References

[1] D. G. White, *Int'l J. Powder Metallurgy*, **37** (2001), 36.

[2] M. M. Avedesian and H. Baker, Editors, *ASM specialty handbook, magnesium and magnesium alloys*, ASM International, Materials Park, OH, (1999).

[3] G. J. Kipouros, Bringing Magnesium to Automobiles, *Materials Solutions for Environmental Problems*, The Metallurgical Society, The Canadian Institute of Mining, Metallurgy and Petroleum , Ed. H. Mostaghasi, Sudbury, Ontario, Canada, August 17–20, (1997), p. 265–267.

[4] E. Ghali, W. Dietzel and K-U. Kalner, *J. Mat. Eng. & Perf.*, **13** (2004), 7–23.

[5] C. J. Bettles and M. A. Gibson, *JOM*, **57** (5) (2005), 46–49.

[6] C. W. Hennessey, W. F. Caley, G. J. Kipouros and D. P. Bishop, *Int'l J. Powder Metallurgy*, **41** (2005), 50–63.

[7] G. J. Kipouros, W. F. Caley and D. P. Bishop, *Met. Mat. Trans. A*, **37A** (12) (2006), 3429–3436.

[8] D. J. Loyd, *Int. Mater. Rev.*, **39**, 1–23 (1994).

[9] H. E. Friedrich and B. L. Mordike, *Magnesium Technology – Metallurgy, Design Data, Applications*, Springer-Verlag, (2006).

[10] W. Xie, Y. Lui, D. S. Li, J. Zhang, Z. W. Zhang and J. Bi, *J. Alloys and Compounds*, **431** (2007), 162–166.

[11] K. Kubota, M. Mabuchi and K. Higashi, *J. Mat. Sci.*, **34** (1999), 2255–2262.

[12] Y. Kawamura and A. Inoue, *Mat. Sci. Forum*, **419–422** (2003), 709–714.

[13] P. Burke, D. Fancelli and G. J. Kipouros, Investigation of the Sintering Fundamentals of Magnesium Powders, Ed. M. O. Pekguleryuz, *Light Metals in Transport Applications*, COM 2007, Toronto, (2007), p.183–195.

[14] P. Burke, D. Fancelli. V. Laverdiere and G. J. Kipouros, *Can. Metall. Q.*, **48** (2) (2009), 123–132.

[15] J. Li, G. J. Kipouros, P. Burke and C. Bibby, Investigation of surface film Formed on Fine Mg Particles, *Microscopy & Microanalysis*, VA, USA, July (2009), p. 26–30.

[16] K. Matsuzaki, K. Hatsukano, K. Hanada, M. Takahashi, T. Shimizu, Mechanical properties and formability of PM Mg-Al based alloys, *Proceedings of the 6th International Conference Magnesium Alloys and Their Applications*, (2005).

[17] W. F. Caley, B. Paton, D. P. Bishop and G. J. Kipouros, *J. Materials Science*, **38** (5) (2003), 1755–1765.

[18] Metal Powders Industries Federation, *Standard Test Methods for Metal Powders and Powder Metallurgy Products*, (1999) Edition.